TURBINE BURNERS: TURBULENT COMBUSTION OF LIQUID FUELS

Final Report
Grant Number FA 9550-06-1-0194

Principal Investigator: William A. Sirignano
Prepared with Derek Dunn-Rankin, Feng Liu,
Ben Colcord, and Sri Puranam

Department of Mechanical and Aerospace Engineering
University of California, Irvine 92697-3975

Objectives

This theoretical/computational and experimental study addressed the vital two-way coupling between combustion processes and fluid dynamic phenomena associated with schemes for burning liquid fuels in high-speed, accelerating, and turning transonic turbulent flows. A major motivation for this type of combustion configuration was the demonstrated potential for improvements in the performance of gas turbine engines via combustion in the turbine passages. This program addressed various fundamental issues concerning combustion in an axially and centrifugally accelerating flow. The major combustion challenge involved ignition and flame-holding of a flame in the high-acceleration flow and the associated optimization of the injection of the fuel and some secondary air into a protected recirculation zone provided by a cavity. The objectives were to advance our understanding of liquid-fuel combustion in accelerating flows and thereby to contribute to the development of turbine-burner technology.

Introduction

Two-way coupling between combustion processes and fluid dynamic phenomena associated with burning fuels in high-speed, accelerating, and turning turbulent flows has been examined both experimentally and computationally. Distinctions between the transonic case of interest

Report Documentation Page

Form Approved
OMB No. 0704-0188

1. REPORT DATE	2. REPORT TYPE	3. DATES COVERED
14 SEP 2009		**01-03-2006 to 31-05-2009**

4. TITLE AND SUBTITLE	5a. CONTRACT NUMBER
Turbine Burners: Turbulent Combustion of Liquids Fuels	5b. GRANT NUMBER
	5c. PROGRAM ELEMENT NUMBER
6. AUTHOR(S)	5d. PROJECT NUMBER
	5e. TASK NUMBER
	5f. WORK UNIT NUMBER
7. PERFORMING ORGANIZATION NAME(S) AND ADDRESS(ES) **Department of Mechanical and Aerospace Engineering,University of California,Irvine,CA,92697**	8. PERFORMING ORGANIZATION REPORT NUMBER
9. SPONSORING/MONITORING AGENCY NAME(S) AND ADDRESS(ES)	10. SPONSOR/MONITOR'S ACRONYM(S)
	11. SPONSOR/MONITOR'S REPORT NUMBER(S)

12. DISTRIBUTION/AVAILABILITY STATEMENT
Approved for public release; distribution unlimited

13. SUPPLEMENTARY NOTES

14. ABSTRACT

15. SUBJECT TERMS

16. SECURITY CLASSIFICATION OF:			17. LIMITATION OF ABSTRACT	18. NUMBER OF PAGES	19a. NAME OF RESPONSIBLE PERSON
a. REPORT	b. ABSTRACT	c. THIS PAGE			
unclassified	**unclassified**	**unclassified**	**Same as Report (SAR)**	**27**	

in this program and previous supersonic studies with cavity injection are discussed. Two-dimensional, non-accelerating, reacting computational results and reacting, accelerating, and turning experimental results have provided insight into the combined combustion and fluid dynamic processes, specifcally the role of the cavity dimensions, Reynolds number, and injection confguration on the flow and flame stability. The Rossiter rules for the frequency of vortex shedding are demonstrated to not apply when injection of a fluid into the cavity occurs, with or without chemical reaction. Both numerical and experimental results show that the cavity aspect ratio is the most important parameter for flame anchoring and flame penetration into the main channel flow. Effects of the cavity design on flame-holding and burning efficiency are reported for various Reynolds numbers. Distinct combustion regimes are identified at the extremes: burning only in the shear layer flowing over the cavity and burning throughout the cavity. The relations of these regimes to mixing rates are discussed.

Literature Review

Gas-turbine engine designers are attempting to reduce combustor length in order to increase the thrust-to-weight ratio and to widen the range of engine operation. One major consequence of the shorter combustor is that the fuel/air residence time can become shorter than the time required to complete combustion; therefore, combustion would occur in the turbine passage. Sirignano and Liu [1] and Liu and Sirignano [2] have shown by thermodynamic analysis that augmentation via burning in the turbine in the aircraft turbojet engine has a number of advantages. It allows for a reduction in length and weight compared to afterburners, a reduction in specific fuel consumption compared to afterburners, and an increase in specific thrust compared to turbojets without augmenters. For the ground-based gas turbine, benefits have been shown by thermodynamic analysis to occur in power/weight and efficiencies [1]. Furthermore, the reduction in peak temperatures due to acceleration results in the promise of reduced pollutant formation and reduced heat transfer losses in many other combustion applications. A mixing and exothermic chemical reaction in the accelerating flow through the turbine passage offers, therefore, an opportunity for a major technological improvement.

One of the challenges involved with mixing and reacting in the turbine passages is the very large three-dimensional acceleration. Sirignano and Kim [3] obtained similarity solutions for laminar, two-dimensional, mixing, reacting and non-reacting layers with a pressure gradient that accelerated the flow in the direction of the primary stream. Fang et al. [4] extended that study to find numerical solutions for an accelerating transonic mixing layer. Mehring et al. [5] further extended this work to include turbulence via a k-ω turbulence model. Cai et al. [6] developed a finite-volume method to include both streamwise and transverse acceleration, while Cheng et al. [7, 8, 9] have used a direct numerical simulation (DNS) to study accelerating transonic mixing layers undergoing transition from laminar to turbulent flows. These works have shown that streamwise acceleration stabilizes both non-reacting and reacting mixing layers.

This study aims to extend these works by considering the injection of fuel into the subsonic portion of the flow, where the flow begins to accelerate. The fuel was injected into a cavity, intended to provide a protected recirculation zone for gaseous-fuel injection, mixing, ignition, and flame-holding to occur. Flows over cavities have been investigated in many previous studies. Rossiter [10] described a feedback mechanism between the flow field and the acoustic field, and derived a semi-empirical formula for the frequencies of vortex shedding at the cavity leading

edge:

$$St_n = \frac{f_n L}{U} = \frac{n - C}{M + 1/\kappa} \tag{1}$$

where St is the Strouhal number, f the frequency, L the cavity length and U the free-stream velocity. C is a correction factor, n is the mode number of oscillation, M is the Mach number, and κ is the ratio of the convective velocity of the vortices to the free-stream velocity. This feedback mechanism is referred to as a shear-layer mode mechanism. Another mode of oscillation, known as the wake mode, was observed by Gharib and Roshko [11] when the length-to-depth ratio of the cavity was increased. This mode was characterized by large vortices developing in the cavity before being ejected with a Strouhal number independent of Mach number. The flow resembled a shedding wake behind a bluff body and was characterized by intense oscillations that were an order of magnitude larger than those observed in shear-layer modes, with a Strouhal number independent of Mach number.

There has been substantially less research performed involving reacting flows with cavities. Most of this work has been motivated by two practical applications. Firstly, cavity-based flameholders have been studied for use in scramjet combustors, with flow Mach numbers typically ranging from 2 to 3. Secondly, cavities have been studied in subsonic flows to provide flame stability in gas-turbine combustors. These combustors have become known as trapped-vortex combustors.

Early research on trapped vortex combustors by Hsu et al. [12, 13] considered gaseous propane and air injected into an axisymmetric cavity to achieve low-speed flame stabilization. Results showed that a vortex is locked in a short cavity with an aspect-ratio $L/D < 1$ and stable flames resulted for cavity lengths between 0.45 and 0.65 of the upstream wall diameter. Longer cavities produced unstable flames, whereas shorter cavities lacked enough volume for flameholding. Similar results showing a limited L/D range for a stable flame zone were obtained by Katta and Roquemore [14, 15] from time-dependent CFD calculations, also with gaseous propane as the fuel. The main conclusions from these low-speed cavity flameholder studies can be summarized as follows:

1. When a vortex is trapped in a cavity, very little fluid is entrained into the cavity from the main flow. Since continuous mass exchange between the cavity and main flow is required for flame stabilization, this problem needs to be overcome by injecting fuel and air directly into the cavity.

2. When air and fuel are injected so that the vortex is reinforced and the mass transfer of the reactive gases into the freestream is increased, the flame stabilization of the cavity is enhanced.

3. In non-reacting flows, a stable cavity flow occurs at a cavity dimension ($L/D = 0.6$) that minimizes the pressure drop. This configuration is also the optimal cavity length for providing the most stable flame.

4. The optimum length-to-depth ratio of the cavity is larger in cases with fluid injection into the cavity than those without injection.

The design of a cavity-based flameholder for supersonic combustors poses a similar problem to that of the turbine burner: the relatively long ignition delay time of liquid hydrocarbon

fuel could exceed the residence time. In both cases, overcoming this problem requires fast evaporation of liquid spray, effective fuel-air mixing and ignition, and stable combustion.

Supersonic combustors typically consider longer cavities with $L/D > 1$. For high speed flows, cavities can generally be divided into two categories: open or closed. In open cavity flows, the shear layer formed at the upstream corner spans the entire cavity length and reattaches along the back face. Conversely, closed cavities occur when the shear layer is unable to span the cavity length and reattaches on the floor of the cavity. The length-to-depth aspect ratio separating open and closed cavities at high speeds is typically from 10 to 12 [16]. Both the shear-layer mode and the wake mode occur only for open cavities.

In studies at the Air Force Research Laboratory, the effectiveness of cavities for flame stabilization in high speed flows was examined. Numerical simulations [17, 18, 19] of non-reacting cavity flows showed that cavity residence times decreased in longer cavities and cavities with slanted downstream walls. The cavity residence time is the time scale associated with the emptying of the cavity by mass exchange with the main flow. This residence time was determined numerically by tagging the fluid in the cavity and monitoring its decay. These studies showed that for cavities of fixed length, the residence time is approximately proportional to the depth, whereas for cavities of fixed depth, the residence time decreases with increased cavity length; therefore, the length of the cavity determines the mass exchange rate between the channel and the cavity, while the cavity depth determines the residence time. Additionally, Davis and Bowersox [17, 18] used their results to obtain an empirical equation for the required depth of the cavity: $D = \tau_r U_\infty / 40$, where τ_r is the required residence time for ignition and U_∞ is the freestream velocity.

Yu et al. studied the influence of the cavity geometry on the combustion of ethylene [20] and kerosene [21, 22, 23] fuel injected upstream of the cavity in a Mach 2 flow and showed that small aspect ratio cavities provide better flameholding than longer cavities. They also combined a short open cavity with a downstream closed cavity, which was demonstrated to have a higher combustion efficiency than a single open cavity. In this configuration, the short open cavity acted as a flameholder, while the downstream closed cavity increased the mixing. Gruber et al. [24] showed that injection of ethylene fuel directly into the cavity is preferable to passive entrainment for providing a uniform fuel-air mixture and for maintaining a stable flame.

Numerical studies by Kim et al. [25] showed that increasing the angle of the downstream cavity wall increased the combustion efficiency, but also increased the total pressure loss. Both combustion efficiency and total pressure loss were shown to increase with the cavity length-to-depth ratio in the range $L/D = 2$ - 4.

Rasmussen et al. [26] studied the effects of a cavity on stability limits in supersonic flow. They showed that injecting fuel from the downstream wall or ramp gave better performance near the lean blowout limit, while injecting from the floor of the cavity gave more stable flames near the rich limit. They also showed that between Mach 2 and Mach 3 the lean blowout limit did not change significantly, whereas the Mach number had a measurable effect near the rich limit.

The above findings, although performed for supersonic flow, provide some guidance for our own research on subsonic cavity flow.

Accomplishments / New Findings

Numerical Results

This research considered flow accelerating from low subsonic speeds up to high subsonic or low supersonic speeds. The presence of the cavity also created a low-speed region and stagnation point flow. This wide range of Mach numbers created numerical difficulties because different numerical schemes perform better at different Mach number ranges and can perform poorly outside of this range. Two numerical schemes have been used in this research [27, 28, 29, 30, 31, 32]. The first scheme was the derivative of an incompressible code that used a pressure-correction equation derived from the continuity equation to solve for the pressure field. In this code, the density varied with temperature and species composition but not with the pressure. This limited variation is suitable for low Mach number flows, such as occur near the channel inlet and inside the cavity. This scheme has been used primarily to look at the effect of the cavity and has not considered the effects of a turning, converging channel. However, at higher Mach numbers, the effect of the pressure change on the density is no longer negligible. The second scheme, for high Mach number flows, instead used the continuity equation directly to solve for the density and the equation of state to calculate the pressure. This scheme is better suited to accelerating flows, where the exit velocity is transonic, and also to turning flows, where the pressure variation across the channel is an important effect.

The describing equations for this problem are the two-dimensional, unsteady, compressible Navier-Stokes equations together with energy and species concentration equations.

$$\frac{\partial \rho}{\partial t} + \frac{\partial}{\partial x_j}(\rho u_j) = 0, \tag{2}$$

$$\frac{\partial}{\partial t}(\rho u_i) + \frac{\partial}{\partial x_j}(\rho u_j u_i) = -\frac{\partial p}{\partial x_i} + \frac{\partial \tau_{ij}}{\partial x_j}, \tag{3}$$

$$\frac{\partial}{\partial t}(\rho E) + \frac{\partial}{\partial x_j}(\rho u_j H) = \frac{\partial}{\partial x_j}\left(k\frac{\partial T}{\partial x_j} + u_i\tau_{ij} + \sum_{m=1}^{N} \rho h_m D_{1m}\frac{\partial Y_m}{\partial x_j}\right) + Q_F\dot{\omega}_F, \tag{4}$$

$$\frac{\partial}{\partial t}(\rho Y_m) + \frac{\partial}{\partial x_j}(\rho u_j Y_m) = \frac{\partial}{\partial x_j}\left(\rho D_{1m}\frac{\partial Y_m}{\partial x_j}\right) + \dot{\omega}_m. \tag{5}$$

The stress tensor in these equations is given by:

$$\tau_{ij} = 2\mu\left[\frac{1}{2}\left(\frac{\partial u_i}{\partial x_j} + \frac{\partial u_j}{\partial x_i}\right) - \frac{1}{3}\frac{\partial u_k}{\partial x_k}\delta_{ij}\right], \tag{6}$$

and the total energy per unit mass is:

$$E = H - \frac{p}{\rho} = h + \frac{1}{2}\left(u^2 + v^2\right) - \frac{p}{\rho}. \tag{7}$$

The enthalpy is calculated from

$$h = \sum_{m=1}^{N} Y_m h_m = \sum_{m=1}^{N} Y_m \int_{T_0}^{T} c_{pm} dT, \tag{8}$$

where c_{pm} is the specific heat at constant pressure of species m, which is calculated as a function of temperature using curve-fitted polynomials. Thermal conductivity k and dynamic viscosity μ for each species are calculated in a similar manner, with the overall value being a mass-weighted average. The binary diffusion coefficients D_{1m} are modeled as functions of pressure and temperature [33], and each species is assumed to be diffusing in nitrogen, the dominant species.

The equation of state for a perfect gas relates the density to the pressure and temperature. For low Mach number calculations, the variation in pressure is caused predominantly by changes in the temperature and species composition. A modified equation of state for a perfect gas can then be used for the low Mach number scheme:

$$\rho = \frac{p}{RT} \approx \frac{p_0}{RT}, \tag{9}$$

where p_0 is a reference pressure rather than a local pressure. The high Mach number code does not use this approximation. The average gas constant R is given by

$$R = \sum_{m=1}^{N} \frac{R_u Y_m}{W_m}. \tag{10}$$

Although high Reynolds numbers were considered, no turbulence modelling has been used because the flow is transitional, rather than fully developed, turbulence.

Benchmarking calculations were first performed for nonreacting flow over a cavity in a straight channel. The flow here was incompressible and isothermal, and the low Mach number numerical code was used. The boundary conditions were constant, uniform inlet velocity; no-slip at all of the walls; constant, uniform pressure at the exit; and zero-valued first spatial derivatives normal to the exit plane of both velocity components.

L	D	Re	St	n
1	1	10,000	1.47	3
1	1	20,000	1.68	3
1	1	40,000	0.58	1
1.5	1	10,000	1.05	2
1.5	1	20,000	0.48	1
2	1	10,000	0.57	1
2	1	20,000	0.73	2
2	0.5	5,000	0.28	wake mode
2	0.5	10,000	0.25	wake mode

Table 1: Strouhal and mode numbers for various cavity sizes and Reynolds numbers

Results without injection in unsteady flows at higher Reynolds number for different cavity sizes are summarized in Table 1. The length L and depth D of the cavity were normalized by the height of the channel, and the Reynolds number was based on the channel inlet height and velocity. The Strouhal number was calculated from the dominant observed shedding frequency, which correlates to the n-th Rossiter mode. For the cases with $L = 2$ and $D = 0.5$, wake modes were observed and Rossiter's formula did not apply.

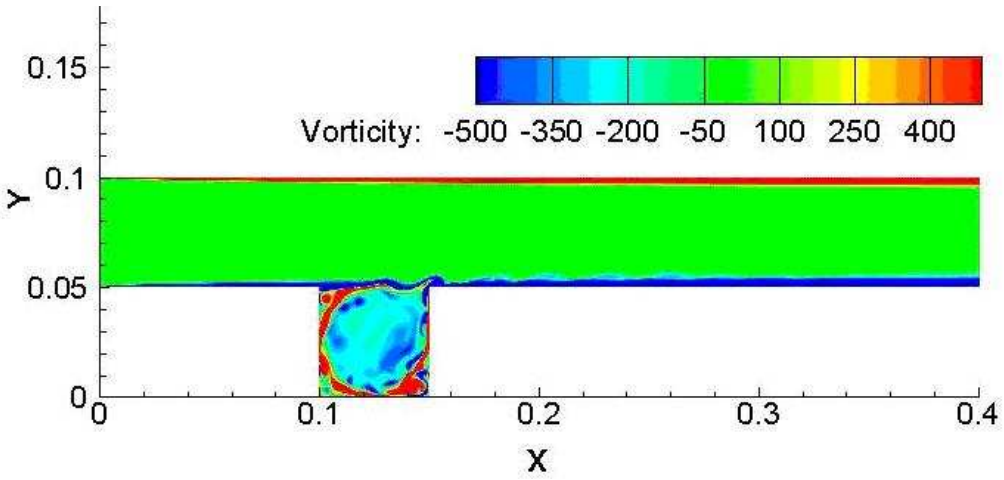

Figure 1: Vorticity contours for $Re = 10,000$ with $L/D = 1$

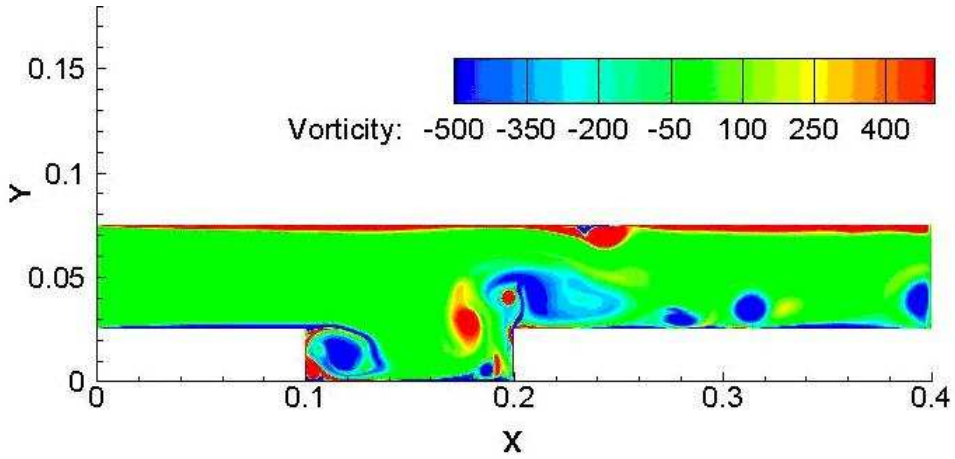

Figure 2: Vorticity contours for $Re = 10,000$ with $L/D = 4$

Significant differences between the shear-layer mode and the wake mode can be seen in the vorticity contours of Figure 1 and Figure 2. The inlet Reynolds numbers are the same for these two cases. Figure 1 shows a case with a square cavity of $L/D = 1$. A single large vortex fills the cavity, and the vorticity in the shear layer is confined to the boundary layer downstream of the trailing edge of the cavity.

With $L/D = 4$, a wake mode developed, as shown in Figure 2. A large vortex can be seen forming near the leading edge of the cavity, while an ejected vortex can be seen downstream of the cavity. This vortex was ejected far enough into the channel to affect the boundary layer on the top wall. These nonreacting flows without injection indicate that the aspect ratio of the cavity has a significant impact on the fuel - air mixing in the cavity. A cavity with a higher aspect ratio is expected to promote mixing better than a deep cavity.

When air was injected steadily into the cavity from the upstream wall, unsteadiness was found to occur at $Re \approx 950$. Without injection, the flow was steady at $Re = 2000$. The mass flow of fluid injected into the cavity iwas 10% of the mass flow in the main channel. Simulations of the same injection flow rate into a quiescent field showed that the jet alone was steady, implying

that there was a coupling between the channel flow and the injection that caused transition to occur at lower Re. With the mass ratio fixed at 10%, the Strouhal number was close to a constant value of 2.0 for $Re = 5000 - 10000$ and for two aspect ratios of $L/D = 1.0$ and $L/D = 2.0$. The injection disrupts Rossiter's feedback mechanism and the oscillation frequency is instead determined by the interaction between the jet and shear layer instabilities; therefore, Rossiter's formula no longer applies.

The reacting flow calculations solve the unsteady, compressible Navier-Stokes equations along with the energy equation and multiple species equations. Gaseous n-heptane has been used as the fuel for the current calculations. The combustion is described as a one-step overall chemical reaction:

$$C_7H_{16} + 11(O_2 + 3.76N_2) \longrightarrow 7CO_2 + 8H_2O + 41.36N_2 \tag{11}$$

and the chemical kinetics rate for the fuel is estimated by

$$\dot{\omega}_F = -A\rho^{a+b}Y_F^a Y_O^b e^{-E_a/R_u T}, \tag{12}$$

where the chemical rate constants $A = 1.2 \times 10^9$, $a = 0.25$, $b = 1.5$, and $E_a = 1.255 \times 10^8$ have been obtained from Westbrook and Dryer [16].

The overall combustion efficiency for the unsteady calculations is defined as:

$$\eta_c = \frac{1}{T}\int_{t_0}^{t_0+T} \frac{\dot{m}_{F,in} - \dot{m}_{F,out}}{\dot{m}_{F,in}} dt, \tag{13}$$

where $\dot{m}_F$ is the fuel mass flow rate into or out of the system. The combustion efficiencies for the cases with gaseous heptane injected from the upstream wall of the cavity are summarized in Table 2.

L	D	Re	η_c
2	1	500	0.34
2	1	1,000	0.32
2	1	2,000	0.61
1	1	5,000	0.30
2	1	5,000	0.60
1	1	10,000	0.40
2	1	10,000	0.71

Table 2: Combustion efficiencies for cavities with gaseous heptane injection

In the reacting results presented here, gaseous heptane fuel was injected into the cavity at an overall equivalence ratio of 1.0 with the air flowing into the main channel. The air inflow and fuel injection temperatures were $1000K$ and $300K$, respectively. The walls of the channel and cavity were isothermal, fixed at $600K$. At an inlet Reynolds number of 1000 and with fuel injected from the center of the upstream wall of a cavity with $L/D = 2$, as shown in Figure 3, 32% of the injected fuel was burned before exiting the channel. This percentage had a slight increase over the burning efficiency of 28% achieved by injecting directly into a channel without a cavity. In the case with the cavity, the flow above the flame and the flame itself were steady. Some unsteadiness still occurred inside the cavity and in the boundary layer beneath the flame.

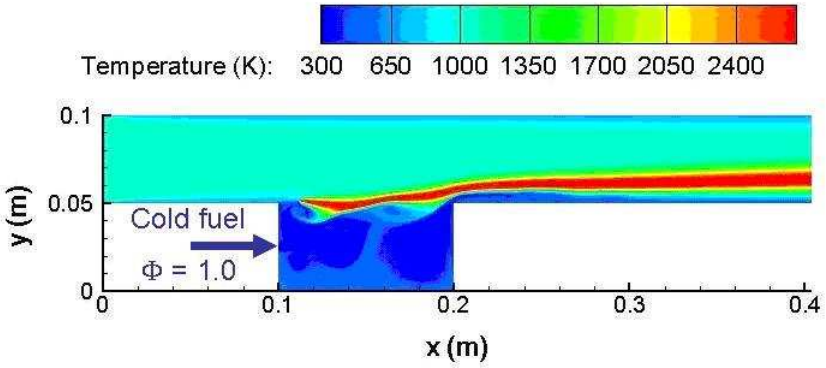

Figure 3: Fuel injection from the upstream wall at $Re = 1000$

For the same cavity size and injection configuration but with $Re = 500$, the burning efficiency increased to 34% due to the increased residence time in the channel. The burning efficiency also increased when the Reynolds number was increased to 2000. This efficiency increased because the downstream portion of the flame became unsteady, as shown in Figure 4, resulting in greater mixing. In this case, 61% of the fuel was burned before leaving the channel. Although the flame had become unsteady downstream, the anchor point of the flame was still stable.

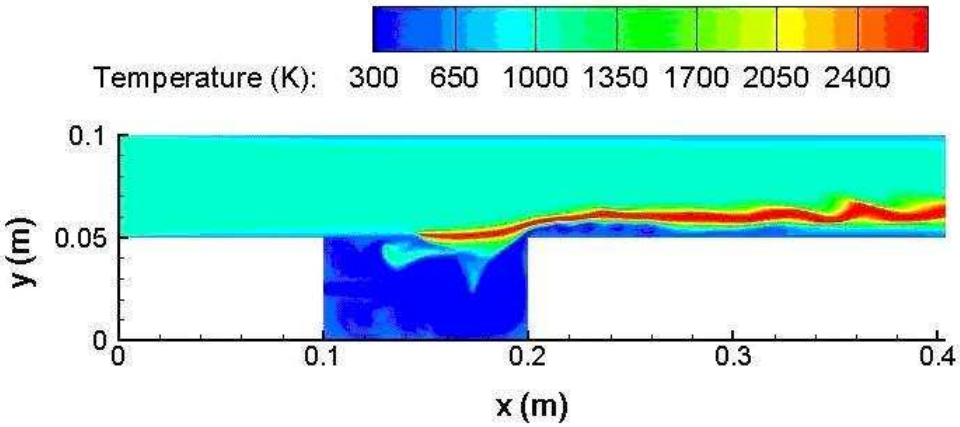

Figure 4: Fuel injection from the upstream wall at $Re = 2000$

At higher Re, the entire flame became unsteady, including the anchor point. Figure 5 shows temperature and fuel mass fraction contours for a calculation with $Re = 5000$ at two different instants. In this case, an igniter had been used between the fuel and air streams to shorten the calculation time. The igniter was switched off after a flame was established, with the times shown after the igniter was turned off. For approximately $0.15s$ after the igniter was turned off, the flame remains anchored in the upper upstream corner of the cavity, as seen in Figure 5a. This time corresponds to approximately 4.5 channel residence times. While anchored in this position, the burning efficiency was approximately 85%.

Because of the two-dimensional configuration, the fuel acted as a sheet or free film rather than as a round jet, so that air from the channel flow could not enter the cavity beneath the fuel stream easily; however, as seen in Figure 5(b) and Figure 5(d), the fuel stream was

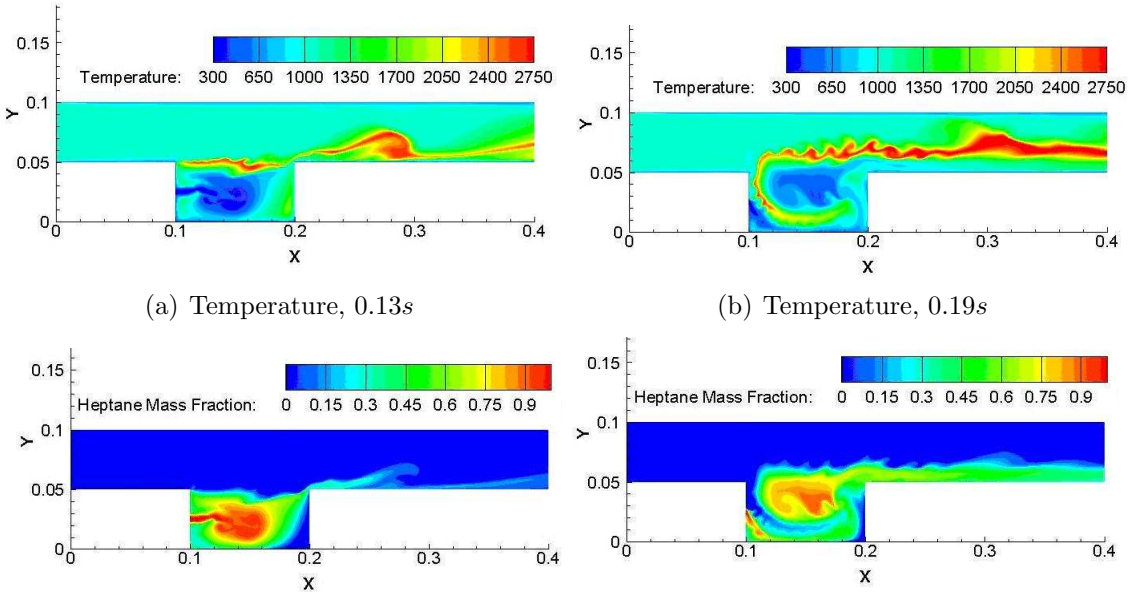

(a) Temperature, 0.13s

(b) Temperature, 0.19s

(c) Heptane, 0.13s

(d) Heptane, 0.19s

Figure 5: Temperature and fuel mass fraction contours 0.13s and 0.19s after igniter is turned off for $Re = 5000$

deflected downwards, allowing air to enter the cavity and the flame to extend around the cavity. Although this air entry increased the air-fuel mixing and the length of the flame, it also caused a displacement of unburned fuel from the cavity into the channel and actually reduced the amount of fuel burned.

The temporal variation of the mass flow rate of fuel entering and exiting is shown in Figure 6. Before the initial downward deflection of the fuel stream at approximately 0.15s, the amount of fuel exiting was relatively constant. After 0.15s, the fuel mass flow rate at the exit fluctuates considerably as the flow became highly unsteady. After 0.4s, approximately 12 channel residence times, the flame was still burning in the vicinity of the cavity. The burning efficiency for this calculation was approximately 60%.

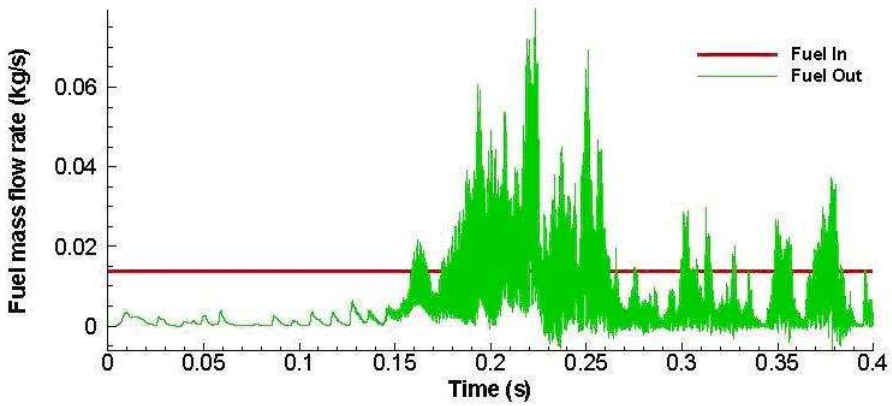

Figure 6: Fuel mass flow rates for a cavity with $L/D = 2.0$ at $Re = 5000$

The same calculation was performed for a cavity with $L/D = 1.0$. For this square cavity, the flame was blown downstream after less than three channel residence times, so that burning occurred only very near the exit of the channel, resulting in a low burning efficiency of approximately 30%. The calculations were also performed with an inlet Reynolds number of $10,000$ for both cavity sizes. The cavity with $L/D = 1$ again had the flame blown downstream, which resulted in a low combustion efficiency of approximately 40%. The longer cavity with $L/D = 2$ showed an improvement in the combustion efficiency over the same cavity at lower Re. The combustion efficiency increased from approximately 60% to 71%. Since the characteristic residence time is inversely proportional to Re, the increase in combustion efficiency occurred despite the characteristic residence time being halved.

The inlet air temperature for all of these reacting calculations was $1000K$. For $Re \leq 2000$, the injected gaseous heptane fuel ignited before exiting the channel, establishing a flame that was anchored in the cavity; however, at $Re \geq 5000$, the fuel did not ignite automatically before exiting and an igniter was switched on until the flame was established. A computation with an extended downstream channel at $Re = 10,000$ showed that ignition occurred approximately 5 channel heights downstream of the cavity.

For all of the reacting calculations, the flow field became much more complex, and there was no clearly identifiable vortex shedding frequency. Neither Rossiter's formula nor the constant Strouhal number observed for the wake mode applied when reaction occurred. This result implies that the unsteadiness of the reaction has a greater impact on the flow field than the mechanisms that create identifiable shedding frequencies.

Computational studies have also been performed on reacting mixing layers in accelerating flows [3, 4, 5, 7] and in turning channels which simulate the turbine stator passage [6, 8, 9]. A mixing layer flowed into the simulated stator passage and hot oxidizing gas flowed on one side of the mixing layer with cold hydrocarbon gaseous fuel on the other side. Cavities have not been used yet in those two-dimensional, unsteady flows where the fluid accelerates from low subsonic speeds to low supersonic speeds, undergoing transition to turbulence. These computations have shown that the reacting flow in the passage results in greater turbulent kinetic energy and mixing as compared to the non-reacting case. Figure 7 shows temperature contours for a calculation with hot air flowing on the outside of the curve, while cold methane gas flows on the inside.

Figure 8 shows a calculation in a channel shape that represents an actual stator passage, including space between the stator and rotor. The same type of behavior as seen in the converging-diverging channel occurred; so, we believe that our experimental studies are relevant.

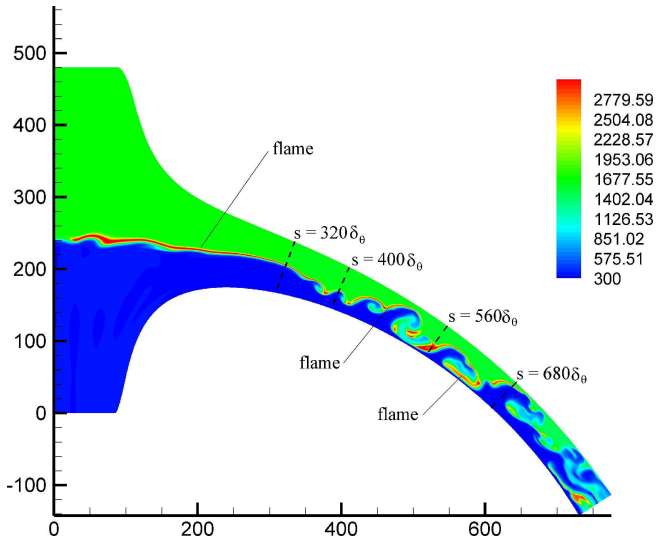

Figure 7: Temperature contours for reacting, accelerating, transonic mixing layer in curved, converging-diverging channel

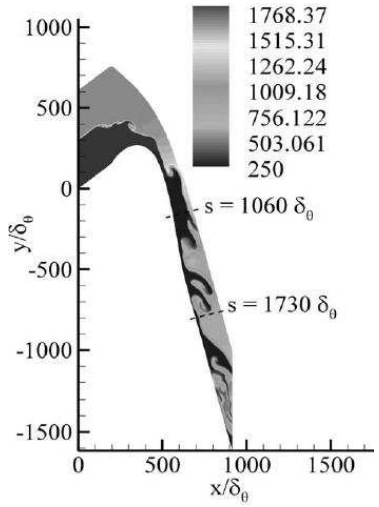

Figure 8: Temperature contours for reacting, accelerating, transonic mixing layer in simulated turbine passage

Experiments

Experiments were conducted in a high speed subsonic combustion facility that was constructed explicitly for use in this project [29, 32, 34]. This unique facility, sketched in Figure 9, had an inlet air system capable of providing an air flow of up to 0.4 m^3/s (24000 l/min). The airflow was measured using three orifice plate flow meters, each of which was calibrated for flow rates not exceeding 0.167 m^3/s (8000 l/min). The air was straightened using a cylindrical settling chamber of 1.6 m length and 0.4 m diameter. The exhaust from the test section was captured and vented from the laboratory using a suction system that had the capacity to handle volumetric flow rates of greater 1 m^3/s. The test section had a rectangular cross-section with

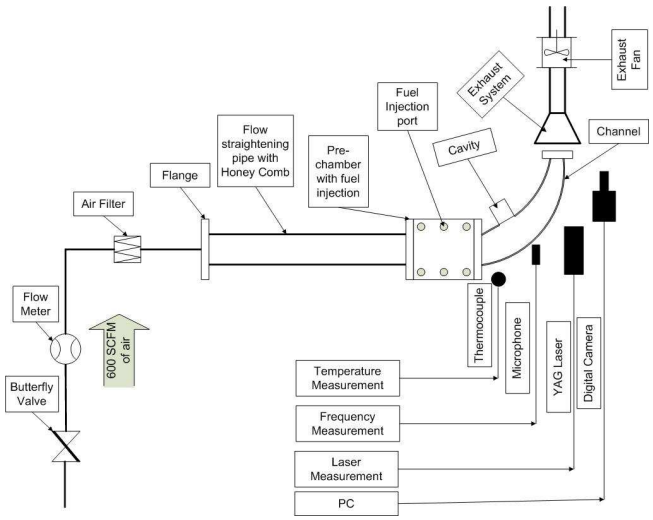

Figure 9: Experiment layout

height variation in the flow direction and a constant width (span normal to Figure 9) of 10 cm. The inlet area was 50 cm^2, and the outlet area was 10 cm^2. The total length of the test section along the centerline arc was 30 cm. The cavity center was placed 5 cm from the inlet along the centerline arc. To provide optical access, one wall of the test section and the cavity base had high temperature glass windows. The flow entering the test section was verified as having a plug flow profile using a pitot tube.

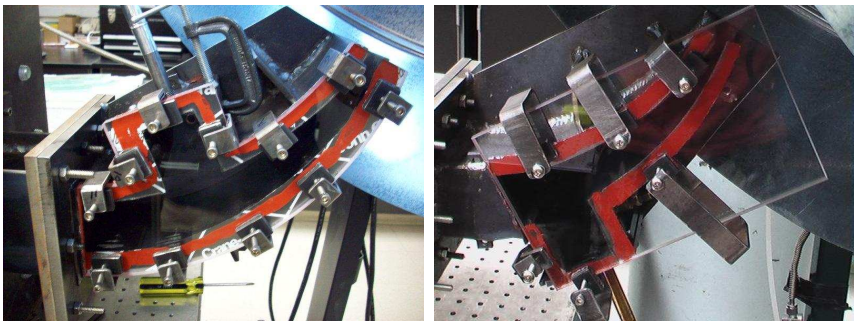

(a) (b)

Figure 10: The two test sections

To study the effect of curvature on flame anchoring, two test sections were used. Both test sections had the same channel curvature and contraction characteristics, as well as the same cavity dimensions and cavity axial location. The only difference was the wall on which the cavity was attached. One test section (Figure 10(a)) had the cavity on the inner wall of the channel, and the other test section (Figure 10(b)) had the cavity on the outer wall of the channel. In addition, each cavity was built such that its depth could be changed to test effects of vortex confinement. For clarity (and because they showed the most substantial differences), the experiments described in this final report only include deep (5 cm) and shallow (2 cm) cavity depths. For each setup, two cavity aspect ratios ($L/D = 1$ and 2.5) were studied. More comprehensive results and configurations will be contained in an M.Eng. thesis [35] and a Ph.D. dissertation [36].

For the cases we concentrate on here, the fuel injection into the test section was accomplished via the cavity. The fuel was injected at various places to find the optimal location. Propane and liquid heptane were used as fuels. The injection location was the same for both liquid and gaseous fuels. For all the results shown, a spark igniter was used inside the cavity to ignite the fuel. The igniter was usually removed once the flame reached a self-sustained condition. Before recording images and temperature data, the test section was allowed to reach thermal equilibrium, which took approximately 5-8 minutes from the start of combustion, depending on the volume of fuel being burnt.

Results - Exit Temperature and Flame Blowout

Temperature was measured at the exit of the test section to determine the extent to which the hot combustion gas was mixed across the main flow. A grid with 4 points along the height of the channel, equally spaced from 0 to 10 mm, and 5 points along the width of the channel, equally spaced from 0 to 100 mm, was used. For every configuration, a temperature surface map was generated and a color bar used to identify the temperature value. A table with the real values of the temperature measured is also included. As a crude measure of energy conversion efficiency ϕ, we computed the ratio between the measured temperature increase and the temperature increase expected under adiabatic conditions:

$$\phi = \frac{T_{real}}{T_{expected}} \times 100 \tag{14}$$

We assume that the heat loss from the cavity and the chamber does not vary substantially so that the difference in thermal energy at the exit is due entirely to changes in the combustion behavior. As shown by the results in Table 3, for deep cavities, more thermal conversion was achieved when the fuel was injected along the main flow direction (i.e., in the downstream direction). Conversely, for shallow cavities, it was more effective to inject fuel against the direction of the main flow. This difference was caused by the substantial variation of vortical structures that was generated by the two cavities. For the deep cavity, there was a single large vortex inside the cavity, and the mixing was improved when the fuel was injected directly into the vortex in a direction reinforcing the vortex. Because the cavity was deep, the residence time for the air and the fuel inside the cavity was relatively long; so some mixing could occur. For shallow cavities, however, there was no single vortex but instead a pair of important vortices that contributed to the combustion behavior. One vortex was near the leading edge of the cavity, and the other occupied a large portion of the cavity. In this case, fuel injected in a

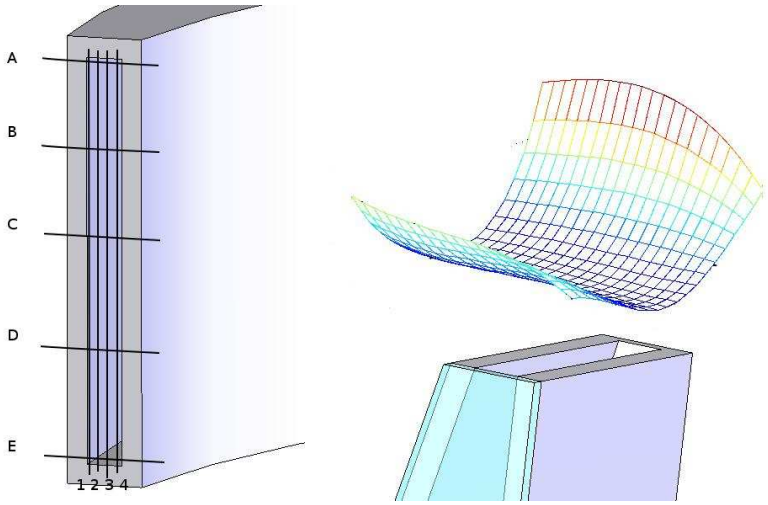

(a) Temperature measurement grid

(b) Example temperature profile

Figure 11: Temperature measurement

direction counter to the main flow was able to mix well in the large vortex even with the relatively short residence time provided by the shallow cavity and gave better mixing. It can also be seen in the table that the influence of the cavity dimension (or aspect ratio) is much more important at higher flow rates. For this higher flow rate condition, the thermal conversion was driven more by the cavity dimension than by the direction of the injection. Interestingly, at all flow rates the flame holding appeared to result from the small vortex at the leading edge of the cavity and this mechanism was not affected by the injection direction or the cavity dimension.

Flame blowout studies were conducted over a wide range of fuel and air flow rates. In these studies, the fuel flow rate was kept constant and the air flow rate was increased from zero to blowout. The lean blowout was noted as the air flow rate at which the flame just blows out. The rich limit was described by the minimum air flow rate necessary for ignition at a given fuel flow rate. From this study an interesting result was observed. For a constant fuel flow rate and an increasing air flow rate the combustion inside the cavity went through three distinct regimes. This three-regime behavior was seen through both inner-wall and outer-wall test-section windows for gaseous fuels with either shallow or deep cavities.

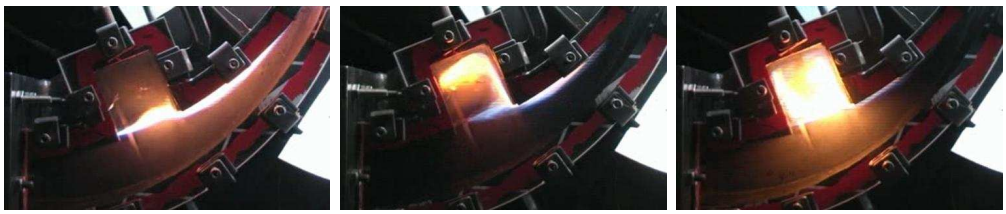

(a) (b) (c)

Figure 12: Three regimes of combustion

Case no.	Fuel flow rate (m^3/s)	Cavity depth	Injection flow direction	Exit temperature increase (K)	Conversion efficiency (%)
1	0.71×10^{-4}	shallow	downstream	60.11	56.10
2	0.71×10^{-4}	shallow	upstream	69.37	64.74
3	0.71×10^{-4}	deep	downstream	60.43	56.40
4	0.71×10^{-4}	deep	upstream	50.34	46.98
5	2.1×10^{-4}	shallow	downstream	166.26	51.72
6	2.1×10^{-4}	shallow	upstream	181.1	56.34
7	2.1×10^{-4}	deep	downstream	129.49	40.28
8	2.1×10^{-4}	deep	upstream	89.5	27.84

Table 3: Description of cases and energy conversion

An example is shown in Figure 12 for the test section with the deep cavity on the inner wall for a fixed propane flow rate of 5×10^{-5} m^3/s. For this case, the operating range was from the rich blowout limit at $Re = 5000$ to the lean blowout limit at $Re = 107{,}000$. At very low air flow rates (Re 5,000-10,000) without large turbulent fluctuations, the flame was confined to the shear layer (Figure 12(a)). This shear layer combustion was expected because very little air entered the cavity at these flow rates, keeping the mixture inside the cavity too rich for combustion. The residence time of air in the main channel was long enough to facilitate mixing along the boundary layer, leading to a long flame anchored at the cavity and extending down the channel. At high air flow rates ($Re > 40{,}000$), most of the combustion occurred in the cavity with significant levels of fluctuation (Figure 12(c)) that appear to come from turbulence. At these air flow rates the local equivalence ratios inside the cavity were within flammability limits throughout the cavity. In addition, at high flow rates, there was almost no combustion outside and downstream of the cavity because the residence times of the air flow outside the cavity were very low (0.012 s) and the global mixture was lean. At moderate air flow rates (Re 10,000 - 40,000), the flame was not stable in the cavity after the igniter was turned off (Figure 12(b)). In this middle regime, the flame appeared to fluctuate between the low speed shear layer diffusion flame and the high speed cavity vortex flame.

For a fixed fuel flow rate the ranges in which the three regimes occurred did not depend on the radial location of the cavity but depended on the cavity aspect ratio. For shallow cavities the transition occurred at a lower Re and the unstable regime spanned a smaller range of flow rates as compared to the deep cavities. The behavior observed in all cavity configurations suggests that the blowout limits and the regimes of cavity combustion are not strongly dependent on the channel curvature but depend strongly on the cavity dimensions and air/fuel flow rates.

To study flame anchoring mechanisms, CH* chemiluminescence imaging experiments were carried out for all configurations. A high speed (Phantom V.3) camera was used to capture images of the flame. The CCD sensor on the camera was covered by a narrowband filter straddling the important chemiluminescence emitted by the excited CH* radical. Since this chemi-excitation occursred almost exclusively in the regions of the flame where there was a high heat release, the bright areas in the images (Figure 13) represent areas of combustion. There was some ambiguity in interpreting chemiluminescence images because the signal was

Aspect ratio / Cavity location	$L/D = 1$	$L/D = 2.5$
Inner wall	Very low: $Re < 11,000$ Very high: $Re > 44,500$	Very low: $Re < 6,500$ Very high: $Re > 28,000$
Outer wall	Very low: $Re < 9,800$ Very high: $Re > 41,000$	Very low: $Re < 5,800$ Very high: $Re > 29,300$

Table 4: Ranges for the three combustion regimes

integrated along the line of sight; however, top views through the auxiliary window in the cavity suggested that the images are a fair representation of the typical reaction zone geometry. In these images there are two distinct regions where combustion is taking place: (1) in the shear layer, including its brief extension along the downstream cavity-side boundary layer, and (2) within the cavity. The images also show that the shear layer reaction zone was spreading as it extended downstream from the leading edge of the cavity and that combustion was nearly uniform in the cavity, particularly for the deep cavity. The images also show that the flame in the shear layer was anchored at the upstream edge of the cavity. Temperature measurements confirmed these findings further. As shown in Figure 14, the temperature within the cavity was fairly uniform. Then there was a noticeable increase followed by rapid decrease in temperature as the probe crossed the shear layer at the top of the cavity and moved into the bulk channel flow.

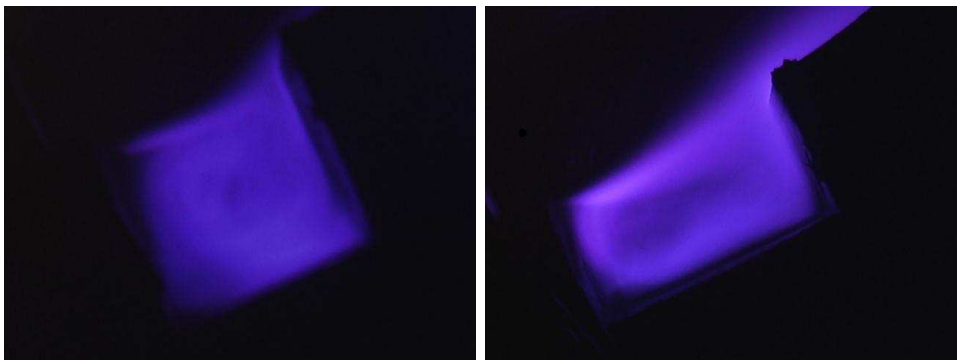

(a) Deep cavity (b) Shallow cavity

Figure 13: CH* Chemiluminescence

From the preceding results (and those from the many redundant additional cases not shown), the following observations were made:

1. Injection location has an effect on the absolute values of temperatures and thermal conversion efficiency, but the qualitative behavior of the flame holding was not affected.

2. The combustion in the shear layer was a diffusion flame, with fuel coming from inside the cavity, where it was injected, and air coming from the main channel flow. This behavior

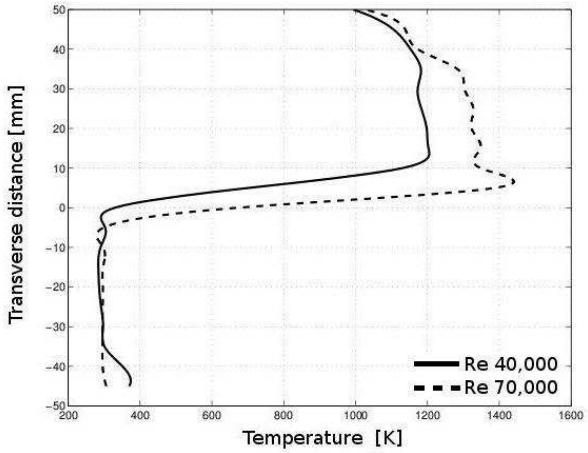

Figure 14: Temperature profile across the cavity

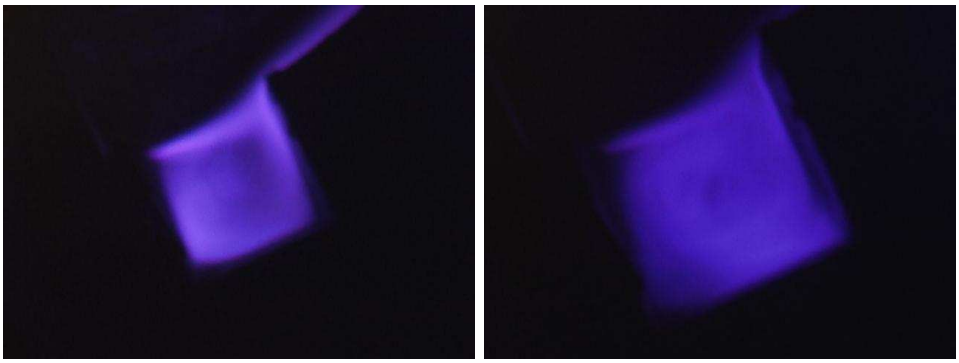

(a) Re = 40,000 (b) Re = 40,000

Figure 15: CH* Chemiluminescence

was clearly observable at low Re, when the combustion was confined to the shear layer (Figure 12(a)).

3. Combustion inside the deep cavity (at high flow rates) approximated that of a stirred reactor. The fuel and air were well-mixed. Combustion proceeded when the mixture equivalence ratio was within flammability limits. Although the combustion was pre-mixed, it was initiated and sustained to some degree by heat transfer (both convection and radiation) from the shear layer. The stirred reactor approximation for the cavity is supported by chemiluminescence images and by the uniform temperature profile measured inside the cavity.

4. At high Re, the percentage of combustion occurring inside the cavity increases and, correspondingly, the percentage of combustion in the shear layer decreases. This can be seen as a change in the relative intensities of the shear layer and the cavity combustion in the CH* images (Figure 15).

In summary, for gaseous combustion there are two distinct combustion zones: the shear layer and the cavity. The shear layer behaves like a diffusion flame and the cavity combustion like

a stirred reactor. The division of overall combustion between the cavity and the shear layer is dependent on the corresponding mixing time scales, specifically, the diffusion time scale in the shear layer and the stirred reactor mixing time scale inside the cavity. As Re increases, the time available for diffusion into the shear layer decreases. Correspondingly, the amount of air entering the cavity increases due to the increase in the shear layer oscillations. This combination of factors produces the gaseous combustion regimes identified above.

Results - Liquid Fuel

Operating the cavity stabilized combustion facility on liquid fuel adds another level of complexity because the fuel must first vaporize before it can mix into the air supply. We found that the evaporation behavior depended fairly critically on the cavity wall temperature, implying that at least a fraction of the liquid fuel was impinging on the cavity walls.

For liquid fuel testing, heptane was used as the fuel, and a typical example using the shallow cavity on the inner wall is shown in Figure 16. A simplex injector was used to inject the fuel into the cavity. The injection point for liquid and gaseous fuels was the same. We used a pilot propane flame to ignite the liquid fuel from a cold start condition. The pilot fuel was injected in the upstream injection port and was ignited with a spark igniter. One of the major differences between the gaseous and liquid fuel combustion was that the liquid fuel combustion was stable only with a shallow cavity. In the deep cavity, the pilot flame was not hot enough to heat the air in the cavity; hence, the evaporation of the liquid fuel was not effective, leading to intermittent combustion. The penetration of the hot gases into the main air flow was better for the liquid case, but heating of the flow was not as uniform. This issue was resolved by using a test section with the cavity on the outer wall. In this configuration, the centrifugal forces help distribute the hot gases across the channel, thereby producing more uniform heating. Despite these somewhat promising results, we did little additional work with liquid fuel because there was too much sensitivity in the system to the relationship between the cavity geometry and the injection nozzle. Wall wetting and subsequent wall evaporation could not be avoided in the confined dimensions of the cavity, so we were never able to achieve a true evaporating spray configuration. Since the gaseous fuel configuration allowed a more complete investigation of the flame structure and the potential for unstable vortices in the cavity to be used for cross-channel mixing of hot product gases, the study focused on these cases (as reported above).

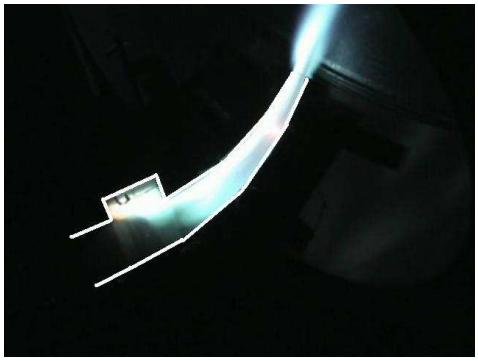

Figure 16: Liquid fuel, Re = 40,000

Discussion of Results

Qualitatively, the experimental and numerical results agree well. Both predict that, for a fixed Reynolds number, the cavity aspect ratio is the most important parameter for flame anchoring and flame penetration into the main channel. Also, both types of results show that, at low Reynolds numbers, combustion occurs mainly in the shear layer between the cavity and the main channel, regardless of the cavity dimensions. For higher aspect ratio cavities computational and experimental results have shown that combustion occurs primarily in the cavity at higher Reynolds numbers, and experiments have shown that cavity combustion also occurs for cavities with lower aspect ratios if the Reynolds number is sufficiently high. It is proposed that there are two time scales that determine if shear-layer or cavity combustion occurs:

- The residence time of a fluid particle inside the cavity (τ_r)
- The diffusion time across the shear layer (τ_D)

The residence time of a fluid particle inside the cavity is assumed to be related to the amount of mixing and heat transfer that occurs within the cavity. If this time is large compared to the diffusion time, then mixing and ignition are more likely to occur in the cavity itself. The diffusion time across the shear layer can be estimated from the shear layer thickness δ and the mass diffusivity $\mathcal{D}$ as

$$\tau_D = \kappa \frac{\delta^2}{\mathcal{D}}, \tag{15}$$

where κ is an arbitrary constant. Averaging δ across the length of the cavity gives:

$$\delta_{avg} = \frac{1}{L}\int_0^L \delta(x)\mathrm{d}x. \tag{16}$$

The shear layer thickness can be related to the Reynolds using classical shear layer theory, as:

$$\delta_x = x\mathrm{Re}_x^{-\alpha}, \tag{17}$$

where $\alpha = 0.5$ for laminar flow and $\alpha < 0.5$ for turbulent flow. From equations 16 and 17

$$\delta_{avg} = L\mathrm{Re}_L^{-\alpha}, \tag{18}$$

and from equations 15 and 18

$$\tau_D = \kappa\frac{\delta^2}{\mathcal{D}} = \kappa\frac{\delta_{avg}^2}{\mathcal{D}} = \kappa\frac{L^2}{\mathcal{D}}\mathrm{Re}_L^{-2\alpha}. \tag{19}$$

Studies have shown that the residence time inside the cavity is independent of cavity length L and depends only on the depth of the cavity D [19, 37] so that

$$\tau_r \propto D \Rightarrow \tau_r = \frac{D}{V_{arbit}} = \kappa'\frac{D}{U_\infty}. \tag{20}$$

From equations 19 and 20:

$$\frac{\tau_D}{\tau_r} = \kappa_1\left(\frac{L^2}{\mathcal{D}}\right)\left(\frac{U_\infty}{D}\right)\mathrm{Re}_L^{-2\alpha}, \tag{21}$$

or

$$\frac{\tau_D}{\tau_r} = \kappa_1 \left(\frac{L}{D}\right)\left(\frac{\nu}{\mathcal{D}}\right)\left(\frac{U_\infty L}{\nu}\right)\mathrm{Re}_L^{-2\alpha} = \kappa_1 \eta \mathrm{Sc}\mathrm{Re}_L^{\beta}, \tag{22}$$

where η is the aspect ratio, Sc is the Schmidt number, and $\beta = 1 - 2\alpha$. For laminar flow $\beta = 0$, and $\beta > 0$ for turbulent flow. This analysis showed that the ratio of time scales is proportional to the aspect ratio, Schmidt number, and the Reynolds number based on cavity length.

For a fixed cavity aspect ratio at low Re, $\tau_D/\tau_r << 1$, which means that the diffusion time is much smaller than the cavity residence time, so combustion will occur in the shear layer. For high Re, $\tau_D/\tau_r >> 1$, the cavity residence time is much shorter than the diffusion time, so combustion occurs in the cavity. For a cavity with a larger aspect ratio, the transition from shear layer combustion to cavity combustion should occur at a lower Reynolds number. These predicted behaviors were seen qualitatively, both in experiments and in computations.

Conclusions

Two numerical schemes have been developed to simulate injection of fuel into a flow cavity. It is found that mass injection of fuel into the cavity at a steady rate can cause unsteadiness and transition in the channel / cavity flow at lower Reynolds-number values than found for flows without injection into the cavity. Transition occurs in the Reynolds number ranges $2000 - 3000$ without injection and $900 - 950$ with injection.

With gaseous heptane fuel injected from the upstream wall of the cavity, the downstream portion of the flame becomes unsteady at in the range $Re = 1000 - 2000$. This unsteadiness increases the burning efficiency significantly more than reducing the Reynolds number to increase the residence time.

At higher Reynolds numbers, the entire flow field becomes much more violent and unsteady. This behavior increases the mixing and the flame length but also causes packets of unburned fuel to be ejected, overall decreasing the burning efficiency.

The following were the major findings and the corresponding experiments/theory supporting the findings for the experimental part of the turbine program.

1. Non-Reacting flow:

   (a) a vortex of the size of the cavity was entrained in a cavity of aspect ratio 1. This vortex was seen using multiple imaging techniques.

   (b) Schlieren images with He and SF6 showed that any gas injected into the cavity followed a similar path. Gases injected, whether they were heavier or lighter than air, diffused into the shear layer and were mixed with the main air flow.

2. Reacting flow:

   (a) Visualization using a high-speed camera showed that there were fixed flow regimes where combustion inside the cavity was self-sustaining.

   (b) Combustion was anchored at the upstream edge of the cavity. This anchoring was seen clearly when the fuel was shut down. This anchoring point did not change, irrespective of the fuel or air flow rate changes or the regime of combustion.

(c) Three regimes where combustion occurs significantly differently were noticed. The three regimes occurred when the fuel flow rate was kept constant and the air flow rate was increased from an inlet Reynolds number of 1000 to 100,000. Combustion in the very low Re and the very high Re regimes was self sustaining.

(d) The three combustion regimes are dictated by the time scales involved in the respective combustion zones. The combustion in the shear layer always exists in all the flow cases studied. The combustion inside the cavity only exists for high flow rates. This result suggests that the mixing inside the cavity and the mixing in the shear layer occur at different rates.

(e) Combustion in the cavity/channel system is divided into two distinct zones: the combustion in the shear/diffusion layer interfacing the cavity with the channel, and the combustion inside the cavity. The combustion inside the cavity is like a stirred reactor and the combustion in the shear layer is a diffusion flame.

(f) The flow exiting the cavity entered into the channel flow and was affected significantly by the curvature of the channel. For the case with the cavity on the inner radius, the mixing of the combustion gases in the main flow was minimal; hence the temperature pattern factor at the exit is very non-uniform. For the case with the cavity on the outer curvature the combustion gases mix all the way across the channel and the pattern factor was more uniform than the other case. The point of impact of the flame at the cavity for all the air flow rates for a fixed fuel flow rate was exactly the same.

(g) The thermal efficiency of the system, defined as the ratio of measured to expected temperature rise, showed that the efficiency of the system jumped in the parameter space which indicates the three regimes.

Both the experiments and computations have shown that the cavity aspect ratio appears to be the most important controlling parameter for flame anchoring and flame penetration into the main channel and that lesser effects are observed by varying the injection direction. Experiments have also shown that that the fuel flow rate has an even smaller effect. While the effects of these last two factors are limited to small changes in the average temperature and efficiency, the cavity aspect ratio cause a significant modification of the flame structure and concomitant variations of average temperature and energy conversion efficiency. The effects can be summarized as follows:

(a) The cavity aspect ratio affected the penetration of the flame in the main channel. A shallow cavity was better because it could push the high-temperature gas further into the main air flow and is better for obtaining a more uniform temperature profile at the exit section.

(b) The fuel injection direction modified the main anchoring point of the flame. When counter flow injection was used, the flame anchored at the cavity's back wall. Otherwise the flame was anchored at the cavity front wall.

(c) The fuel flow rate modified only the amount of heat released by the combustion, which was seen as an effective increase in temperature at the exit. It did not affect the flame stability, the flame shape inside the cavity, or the flame anchoring point.

Personnel Supported

Professor William A. Sirignano
Professor Derek Dunn-Rankin
Professor Feng Liu
Graduate Student Researcher Ben Colcord
Graduate Student Researcher Sri Puranam
Graduate Student Researcher Felix Cheng
Visiting Student Researcher Jonathan Arici

Publications

F. Cheng, F. Liu, and W. A. Sirignano, "Nonpremixed Combustion in an Accelerating Turning, Transonic Flow Undergoing Transition," AIAA Journal, Vol. 46, pp. 1204-15, 2008.

S. V. Puranam, J. Arici, N. Sarzi-Amade, D. Dunn-Rankin, and W. A. Sirignano "Combustion in a Curving, Contracting Channel with a Cavity Stabilized Flame," Proceedings of The Combustion Institute, Vol. 32, pp. 2973-81, 2009.

F. Cheng, F. Liu, and W. A. Sirignano, "Reacting Mixing-Layer Computations in a Simulated Turbine-stator Passage," J. of Propulsion and Power 25, No. 2, 2009.

B. Colcord, F. Liu, and W. A. Sirignano, "Flame-Holding with Fuel Injection into Cavity Adjacent to Air Channel," J. of Propulsion and Power, in preparation, 2009.

Interactions

Seminars at University of Connecticut and Rensselaer Polytechnic Institute, W. A. Sirignano.

"Turbine-burner Research," presented at Panel Session on "Advanced Compact Combustor Technologies," 2008 AIAA Aerospace Sciences Meeting, Reno, NV., W. A. Sirignano.

"Secondary Air Injection in a Miniature Film Combustor, and other topics," Hiroshima University, Hiroshima, Japan, December 10, 2008, D. Dunn-Rankin.

"Graduate Research in the LFA Group," Osaka University, Osaka, Japan, December 8, 2008, D. Dunn-Rankin.

"Using Old Fuels in New Ways," Aoyama Gakuin University, Tokyo, Japan, November 28, 2008, D. Dunn-Rankin.

"Lasers, Flames and Aerosols: recent results in combustion research," Keio University, Yokohama, Japan, November 27, 2008, D. Dunn-Rankin.

"Recent Combustion Research in Lasers, Flames, and Aerosols," University of California,

Riverside, Departmental Seminar, October 10, 2008, D. Dunn-Rankin.

"Lasers, Flames, and Aerosols: introduction to research in combustion at UCI," Universidad Nacional Estadio Sao Paulo (UNESP), Brazil, July 10, 2008, D. Dunn-Rankin.

"Lasers, Flames, and Aerosols: current combustion research at UCI," Universidad Federal Rio de Janeiro, Brazil, July 8, 2008, D. Dunn-Rankin.

Interactions with Dr. Joseph Zelina and Dr. Mel Roquemore of Air Force Research Labs.

New Discoveries

No patents or inventions. New understandings and new data are presented in body of report.

Honors / Awards

W. A. Sirignano, Sustained Service Award, 2006, American Institute of Aeronautics and Astronautics.

W. A. Sirignano, First Dusinberre Lecture, Pennsylvania State University, April 10, 2007, "Advances in the Theory of Liquid-Fuel Burning."

W. A. Sirignano, Plenary Lecture, Seventh International Symposium on Special Topics in Chemical Propulsion: Advancements in Energetic Materials and Chemical Propulsion, Kyoto, Japan, September, 2007, "Recent Theoretical Advances for Liquid-fuel Atomization and Burning."

W. A. Sirignano, Wyld Propulsion Award, 2009, American Institute of Aeronautics and Astronautics. *Citation; "For extensive and fundamental contributions to the advancement of chemical rocket propulsion through theories of nonsteady combustion and fluid dynamics."*

W. A. Sirignano, Society for Industrial and Applied Mathematics Fellow, 2009. *Citation; "For contributions to fluid dynamics, combustion theory, and their applications to propulsion."*

References

[1] W. A. Sirignano and F. Liu, "Performance increases for gas-turbine engines through combustion inside the turbine," *Journal of Propulsion and Power*, vol. 15, no. 1, pp. 111–118, 1999.

[2] F. Liu and W. A. Sirignano, "Turbojet and turbofan engine performance increases through turbine burners," *Journal of Propulsion and Power*, vol. 17, no. 3, pp. 695–705, 2001.

[3] W. A. Sirignano and I. Kim, "Diffusion flame in a two-dimensional, accelerating mixing layer," *Physics of Fluids*, vol. 9, no. 9, pp. 2617–2630, 1997.

[4] X. Fang, F. Liu, and W. A. Sirignano, "Ignition and flame studies for an accelerating transonic mixing layer," *Journal of Propulsion and Power*, vol. 17, no. 5, pp. 1058–1066, 2001.

[5] C. Mehring, F. Liu, and W. A. Sirignano, "Ignition and flame studies for an accelerating transonic turbulent mixing layer," *AIAA Paper 01-0190*, 2001.

[6] J. Cai, O. Icoz, F. Liu, and W. A. Sirignano, "Ignition and flame studies for an accelerating transonic mixing layer in a curved duct flow," *AIAA Paper 01-0180*, 2001.

[7] F. Cheng, F. Liu, and W. A. Sirignano, "Nonpremixed combustion in an accelerating transonic flow undergoing transition," *AIAA Journal*, vol. 45, no. 12, pp. 2935–2946, 2007.

[8] F. Cheng, F. Liu, and W. A. Sirignano, "Nonpremixed combustion in an accelerating turning transonic flow undergoing transition," *AIAA Journal*, vol. 46, no. 5, pp. 1204–1215, 2008.

[9] F. Cheng, F. Liu, and W. A. Sirignano, "Reacting mixing-layer computations in a simulated turbine-stator passage," *Journal of Propulsion and Power*, vol. 25, no. 2, 2009.

[10] J. E. Rossiter, "Wind tunnel experiments on the flow over rectangular cavities at subsonic and transonic speeds," Technical Report 64037, Royal Aircraft Establishment, 1964.

[11] M. Gharib and A. Roshko, "The effect of flow oscillations on cavity drag," *Journal of Fluid Mechanics*, vol. 177, pp. 501–530, 1987.

[12] K.-Y. Hsu, L. P. Goss, and D. D. Trump, "Performance of a trapped-vortex combustor," *AIAA Paper 95-0810*, 1995.

[13] K.-Y. Hsu, L. P. Goss, and W. M. Roquemore, "Characteristics of a trapped-vortex combustor," *Journal of Propulsion and Power*, vol. 14, no. 1, pp. 57–65, 1998.

[14] V. R. Katta and W. M. Roquemore, "Numerical studies on trapped-vortex concepts for stable combustion," *Journal of Engineering for Gas Turbines and Power*, vol. 120, no. 1, pp. 60–68, 1998.

[15] V. R. Katta and W. M. Roquemore, "Study on trapped-vortex combustor - effect of injection on flow dynamics," *Journal of Propulsion and Power*, vol. 14, no. 3, pp. 273–281, 1998.

[16] D. E. Nestler, A. R. Saydah, and W. L. Auxer, "Heat transfer to steps and cavities in hypersonic turbulent flow," *AIAA Paper 68-0673*, 1968.

[17] D. L. Davis and R. D. W. Bowersox, "Stirred reactor analysis of cavity flame-holders for scramjets," *AIAA Paper 97-3274*, 1997.

[18] D. L. Davis and R. D. W. Bowersox, "Computational fluid dynamics analysis of cavity flame-holders for scramjets," *AIAA Paper 97-3270*, 1997.

[19] M. R. Gruber, R. A. Baurle, and T. Mathur, "Fundamental studies of cavity-based flameholder concepts for supersonic combustors," *Journal of Propulsion and Power*, vol. 17, no. 1, pp. 146–153, 2001.

[20] K. Yu, K. J. Wilson, and K. C. Schadow, "Effect of flame-holding cavities on supersonic-combustion performance," *Journal of Propulsion and Power*, vol. 17, no. 6, pp. 1287–1295, 2001.

[21] K. Yu, J. G. Li, X. Y. Chang, L. H. Chen, and C. J. Sung, "Investigation of fuel injection and flame stabilization in liquid hydrocarbon-fueled supersonic combustors," *AIAA Paper 01-3608*, 2001.

[22] K. Yu, J. G. Li, X. Y. Chang, L. H. Chen, and C. J. Sung, "Investigation of kerosene combustion characteristics with pilot hydrogen in model supersonic combustors," *Journal of Propulsion and Power*, vol. 17, no. 6, pp. 1263–1271, 2001.

[23] K. Yu, J. G. Li, X. Y. Chang, L. H. Chen, and C. J. Sung, "Fuel injection and flame stabilization in a liquid-kerosene-fueled supersonic combustors," *Journal of Propulsion and Power*, vol. 19, no. 5, pp. 885–893, 2003.

[24] M. R. Gruber, J. M. Donbar, and C. D. Carter, "Mixing and combustion studies using cavity-based flameholders in a supersonic flow," *Journal of Propulsion and Power*, vol. 20, no. 5, pp. 769–778, 2004.

[25] K. M. Kim, S. W. Baek, and C. Y. Han, "Numerical study on supersonic combustion with cavity-based fuel injection," *International Journal of Heat and Mass Transfer*, vol. 47, pp. 271–286, 2004.

[26] C. C. Rasmussen, J. F. Driscoll, K.-Y. Hsu, J. M. Donbar, M. R. Gruber, and C. D. Carter, "Stability limits of cavity-stabilized flames in supersonic flow," *Proceedings of the Combustion Institute*, vol. 30, pp. 2825–2833, 2005.

[27] B. Colcord and W. A. Sirignano, "Combustion in a flow cavity," in *5th US National Combustion Meeting*, (UC San Diego), March 2007. Poster Paper.

[28] B. Colcord and W. A. Sirignano, "Combustion model with fuel injection into and air flow past a cavity," in *Western States Section/ Combustion Institute Meeting*, (Sandia Laboratories), October 2007.

[29] J. Arici, V. S. Puranam, B. Colcord, D. Dunn-Rankin, and W. A. Sirignano, "Combustion and flameholding in a turbine burner configuration: An experimental and numerical exploration of reacting flow in a curving contracting channel," in *32nd International Combustion Symposium*, 2008. Poster Paper.

[30] B. Colcord, F. Liu, and W. A. Sirignano, "Flame-holding with fuel injection into cavity adjacent to air channel," *Journal of Propulsion and Power*. In preparation.

[31] B. Colcord, F. Liu, and W. A. Sirignano, "Flame-holding with fuel injection into cavity adjacent to air channel," in *6th US National Combustion Meeting*, (Ann Arbor, MI), May 2009.

[32] W. A. Sirignano, D. Dunn-Rankin, F. Liu, B. Colcord, and V. S. Puranam, "Turbine burners: Flameholding in accelerating flow," in *Joint Propulsion Meeting*, (Colorado), 2009.

[33] T. K. Sherwood, *Mass Transfer*. McGraw-Hill, 1975.

[34] V. S. Puranam, J. Arici, and D. Dunn-Rankin, "High speed subsonic test facility for reacting and non-reacting flow studies," in *Western States Section / The Combustion Institute Fall Meeting*, (Irvine, CA), October 2009, submitted.

[35] J. Arici, "Combustion behavior in a model turbine burner," Master's thesis, Politecnico di Milano, expected 2009.

[36] V. S. Puranam, *Combustion in highly accelerating flows*. Ph.D. dissertation, University of California, Irvine, expected 2009.

[37] A. Ben-Yakar and R. Hanson, "Cavity flame-holders for ignition and flame stabilization in scramjets: An overview," *Journal of Propulsion and Power*, vol. 17, no. 4, pp. 943–952, 2001.